

## CHANGES IN ELECTROLYTE TRANSMITTANCE AT 254 nm ACCORDING TO THE STATE OF HEALTH OF LEAD ACID BATTERIES

### CAMBIOS EN LA TRANSMITENCIA DEL ELECTROLITO A 254nm SEGÚN EL ESTADO DE SALUD DE LAS BATERÍAS DE PLOMO

Edwin García QUINTERO<sup>1)</sup>, Jose Alfredo PALACIO-FERNÁNDEZ <sup>\*1,2)</sup>

<sup>1)</sup> Universidad de Antioquia; TESLA research group, Medellín Colombia

<sup>2)</sup> Instituto Tecnológico Pascual Bravo; GIIAM research group, Medellín Colombia

<sup>\*</sup> Corresponding author, E-mail: jose.palaciof@udea.edu.co, josealpa@pascualbravo.edu.co  
DOI: <https://doi.org/10.35633/inmateh-68-59>

**Keywords:** *Electronic Load, Data acquisition, power-IGBT, Battery management, lead acid battery*

#### ABSTRACT

*The estimation of the state of health (SOH) of lead-acid batteries for electrical energy storage is an important factor when planning their replacement and energy management. There are many methods to calculate this parameter. The novelty of this work is that it employs an optical method that produces compelling results showing the variation of the UVC transmittance of the electrolyte when the battery has different SOH levels, which is a novel alternative to the existing one of ampere counting, which is also experimented within this work.*

#### RESUMEN

*La estimación del estado de salud (SOH) de las baterías de plomo-ácido para almacenamiento de energía eléctrica es un factor importante a la hora de planificar su reposición y gestión energética. Hay muchos métodos para calcular este parámetro. La novedad de este trabajo es que emplea un método óptico que produce resultados contundentes mostrando la variación de la transmitancia UVC del electrolito cuando la batería tiene diferentes niveles de SOH, lo cual es una alternativa novedosa a la existente de conteo de amperios, que también es experimentado en este trabajo.*

#### INTRODUCTION

Currently, the global problem linked to the increase of greenhouse gases in the atmosphere such as, for example, the average CO<sub>2</sub> content in the earth's atmosphere, which has increased from 390 ppm in 2011 to approximately 410.19 ppm as of 2018, causing an increase in the temperature of the earth's atmosphere, has manifested itself to a greater degree. This alarming increase in both CO<sub>2</sub> content and its corresponding temperature rise along with finite oil and gas resources have forced mankind to face a challenge and a new opportunity to find different energy sources such as renewable energy sources (Olia et al., 2019), but these sources involve new research to facilitate their positioning. This is how renewable energy sources go hand in hand with battery energy storage systems, which are one of the critical elements that allow the adoption of generation based on renewable sources. A considerable amount of research activities is devoted to the field of batteries, especially with the aim of reducing production costs, increasing their reliability and performance (Ospina Agudelo, Zamboni, & Monmasson, 2021). One of the main indicators that quantify battery performance is known as State of Health (SOH). This indicator is obtained by comparing the current total capacity value of the battery with its initial value (Rezvanizani et al., 2014; Olabi et al., 2021).

The estimation of SOH and other battery performance indicators is a broad research topic with great relevance for all integrated power systems involving batteries of different technologies (Wong et al., 2017; Dey et al., 2014), especially for their energy management and for battery replacement planning. This can be done by experimental analysis or by modelling, the experimental analysis can be by direct or indirect measurement (Xiong et al., 2018).

Hard sulfation is one of the most frequently cited causes of reduced battery performance. In a lead-acid battery, lead sulphate (PbSO<sub>4</sub>) is formed at both electrodes as a natural product of the chemical discharge reaction. This presents a number of problems, the first of which is the fact that some of the active materials become locked up within the inactive lead sulphate, causing a decrease in available capacity (Suozzo, 2008).

<sup>1</sup> Edwin García Quintero, Ph.D.; Jose Alfredo Palacio-Fernández, Ph.D. (c)

Among the experimental methods, the impedance measurement of the battery has been investigated, which increases as the battery wears out or loses its initial current capacity. The internal resistance of the battery does not belong to the external parameters of the battery, strictly speaking, the internal resistance is one of the inherent characteristics of the battery. Most battery management systems take internal resistance parameters as auxiliary parameters for battery condition estimation both to determine the state of charge (SoC) as well as SOH (Wang *et al.*, 2020; Gaouzi *et al.*, 2021). Another method is the counting of charge cycles, which is widely employed in the calculation of SOH of laptop batteries, there are also destructive methods in which the battery is uncovered to internally analyse the state by techniques such as Raman spectroscopy, X-ray diffraction, electron microscopy in which changes in the internal structure are looked at Xiong research (Xiong *et al.*, 2018).

One of the indirect experiments for SOH calculation and which has good accuracy, besides being the most employed to compare the performance of other methods for SOH calculation, is ampere counting, which, to obtain the remaining capacity for charging or discharging, requires long-term monitoring and memorization of the battery current. It is an indispensable process, which costs a lot of time and energy, and the remaining capacity is highly dependent on the high-precision current sensor used to reduce the accumulated error (Berecibar *et al.*, 2016; Rezvanizani *et al.*, 2014). The SOH therefore represents the ratio of the current maximum battery capacity to the maximum capacity before first use and is given in percentages as expressed by equation (1) (Ng *et al.*, 2009).

$$SOH(k) = \frac{Q_{\max}(k)}{Q_{\max\_new}} \quad (1)$$

where  $Q_{\max}$  is the current maximum capacity of the battery in Amperes/hours (Ah) and  $Q_{\max\_new}$  is the maximum capacity in Ah when the battery was new.

The amperage count, which gives the current capacity at cycle K of charging or discharging, is defined by equations (2) and (3) (Rezvanizani *et al.*, 2014).

State of charge during charging:

$$SoC = SoC_0 + \frac{1}{Q_{\max}(k)} \int_0^t |I| dt \quad (2)$$

State of charge during discharge:

$$SoC = SoC_0 - \frac{1}{Q_{\max}(k)} \int_0^t |I| dt \quad (3)$$

Where  $SoC$  is the state of charge of the battery, which increases to the maximum capacity as it is charged according to equation (2) or discharged according to equation (3),  $SoC_0$  is the initial state of charge of the battery and is the nominal capacity at the k charge or discharge cycle.

The discharge process at the experimental level, can be performed by means of an electronic load to which the current rate ( $I$ ) demanded from the battery can be varied and discharged at different rates (Wong *et al.*, 2017).

The value of the integration time  $t$ , changes in each charge discharge cycle and goes up to a value in which the voltage of the battery reaches 10.5 v.

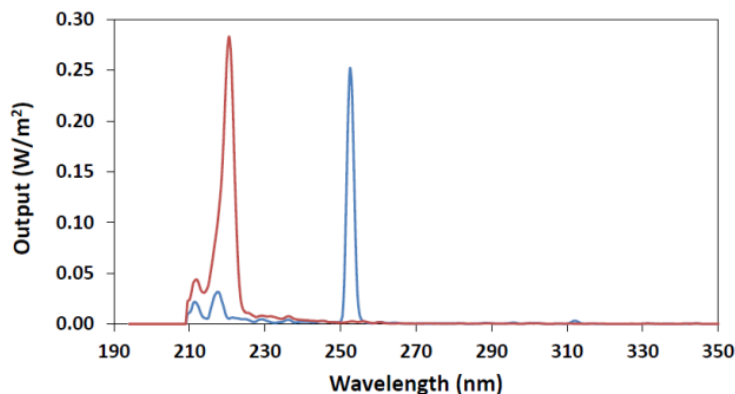
Different characteristics of the battery can be used to identify its SOH, such as capacity and internal resistance, but these are an evaluation and judgment rather than an accurate measurement (Ng *et al.*, 2009).

On the other hand, none of the investigated methods perform analysis by transmittance or absorbance of light in any part of the spectrum in which a variation in the transmittance of the battery electrolyte due to the variation of the battery SOH is observed. Investigations of UVC ultraviolet light are quite widespread, for example in virus disinfection or deactivation processes (Bhardwaj *et al.*, 2021). The most common UVC light sources for many decades have been mercury discharge lamps, especially low-pressure mercury vapour lamps, with a strong emission peak at 254 nm, which is close to the absorption of RNA (Heßling *et al.*, 2020).

Low-pressure mercury lamps are very selective at 254 nm and can be seen in blue in Fig. 1 (Takeda *et al.*, 2021).

Although relevant studies on SOH in batteries have been performed by different methods, no research has been found that relates the reduction of transmittance in the electrolyte of a battery to the prolonged time of use (SOH).

In this study, a method of measuring the SOH of liquid electrolyte lead-acid batteries by counting amperes is designed and constructed in parallel, from a data acquisition system connected to an electronic load that allows manipulating or regulating the battery discharge current, and by means of charge and discharge cycles with thirteen battery decay points or total amperes counting for different SOH and relate it to the percentage of transmittance detected by a sensor at the frequency of 254 nm emitted by a UVC radiation.



source.

**Fig. 1 - Spectral discharge ( $W\ m^{-2}$ ) from a 55-W UV-C (254 nm, low-pressure mercury lamp (blue line) and 250 W 222 nm Krypton Chloride excimer lamp (red line) (Takeda et al., 2021).**

The main objective of this research is to determine the relationship between the SOH measured from a current measurement system that allows the calculation of the total charge of the battery after several charge and discharge cycles, compared with the percentage of transmittance of the electrolyte of 4 lead acid batteries of 42 Ah and 12 V, discharged from 100% of SOH (42 Ah) until it presents 30.5% which is taken as the limit percentage of experimentation due to the long-time of final wear of the batteries of the maximum capacity

## MATERIALS AND METHODS

### Measurement system of the electrical variables

The embedded system performs permanent monitoring of the current to count the amperes consumed until the voltage drops to a certain value where the electronic load as implemented by *García & Palacio, 2020* (*García Quintero & Palacio-Fernández, 2020*), cannot supply the programmed current or the voltage of the active battery reaches approximately 10.5 volts as deep discharge. And the charging process is started again to fulfil a complete cycle. The scheme implemented to charge and discharge the battery under the above conditions is shown in Fig. 2. In this, the electronic charge control measures the voltage across a 100 W, 1 Ohm resistor connected to the output of the IGBT emitter, the battery current is in proportion to the measured voltage. When the battery is discharging the voltage between collector and emitter is reduced to keep the voltage across the RL resistor constant and therefore the current through it as well. The AO comparator serves as a control element on the IGBT gate voltage, which in turn increases or decreases the VCE voltage in the case of discharge. The embedded system captures the current and adjusts the operational amplifier voltages according to the desired current, the analogue to digital conversion resolution used in the data acquisition with the Arduino to record the tests was 10 bits.

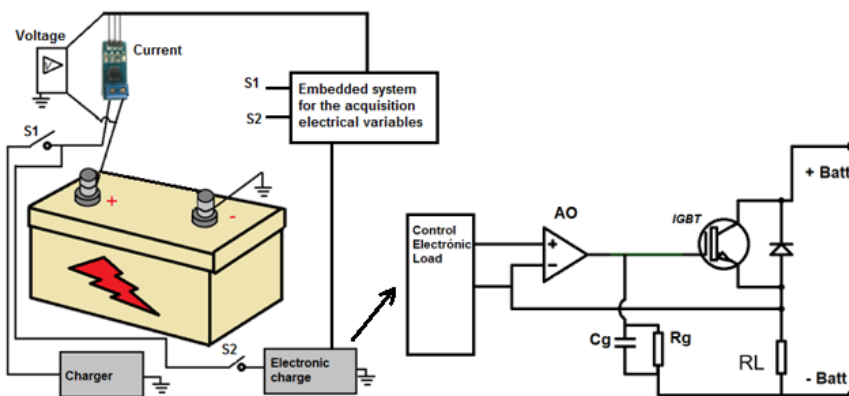


**Fig. 2 - General schematic of the experimental set-up**

The electronic load (fig. 3.a) maintains an almost constant current around 6 Ah (fig.4) and drops a little at the end of the load when the measured voltage is approximately 10.5 volts. The data are obtained from a data acquisition system (Fig. 3.b) consisting of an embedded system based on Arduino Nano, with storage system in microSD and by serial communication with the PC using Matlab®; in addition to a voltage divider system isolated by operational amplifiers that allow measuring voltages higher than 5 volts and lower than 22 volts.

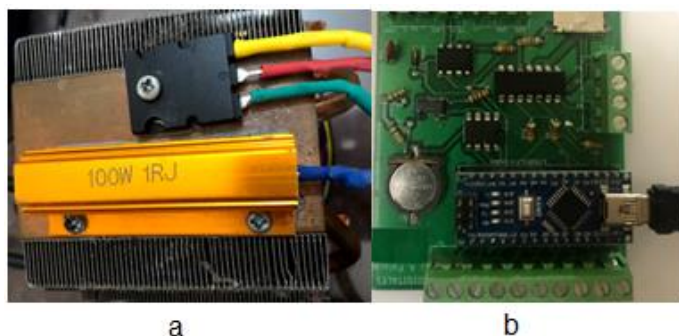


Fig. 3 - a) Electronic load power system and b) Data acquisition system

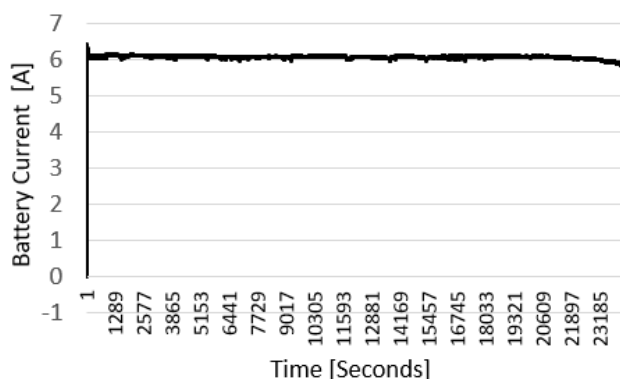


Fig. 4 - Battery discharge current curve taken by the Hall effect sensor.

The developed work considered the analysis for four batteries, whose maximum initial capacity when new is 42 Ah (Ampere-hours). The data are acquired by means of an embedded system and the electronic load is designed from an IGBT as a power control element.

Discharge cycles are performed with a depth of discharge (DoD) of 100%, taking as a base of 100% when the battery drops to a voltage of 10.5 volts. Discharge current was performed at rates of 14.2% of maximum rated capacity, and interleaved discharges of 5% of rated capacity to match the C20 standard which is stated as the maximum load divided by 20, which allows recording the value of the load in the previous cycle of charging and discharging at a higher current.

Discharge tests, as mentioned above, are performed at rates of C3 or 14.2% of the maximum battery capacity. In the case of the 42 Ah batteries, the discharge was performed at 6 amps. It should be noted that this ratio is maintained regardless of the state of health (SOH) by the discharges performed in each cycle, the amperage count is performed by securing the current in the electronic load through the data acquisition system and using equation (1) the SOH is obtained.

### Measurement of UVC

Repeat measurements are taken during the same experimental run that is, they are the measurements taken in each cell in the same run of the experiment, while replicate measurements are taken during identical but separate experimental runs, which are taken in the same SOH run, but for cells 2 to 5 of the battery electrolyte, it is monitored that the electrolyte level during the tests is always above the level of the electrodes.

Fig. 5 shows the internal system of the camera implemented for the transmittance measurement that allows to pass through the electrolyte. It consists of a two wire SHT10 digital interface sensor, which allows measuring temperature values in the range 10°C to 80°C with an accuracy of  $\pm 0.5^\circ\text{C}$ ; a UVC lamp with a narrow spectral range maximized at 254 nm, a quartz cuvette containing the electrolyte to be measured and a 254 nm UVC sensor. The chamber is closed during measurements. The distance between the lamp and the electrolyte is 0.5 cm, and between the electrolyte and the sensor is 1 cm.

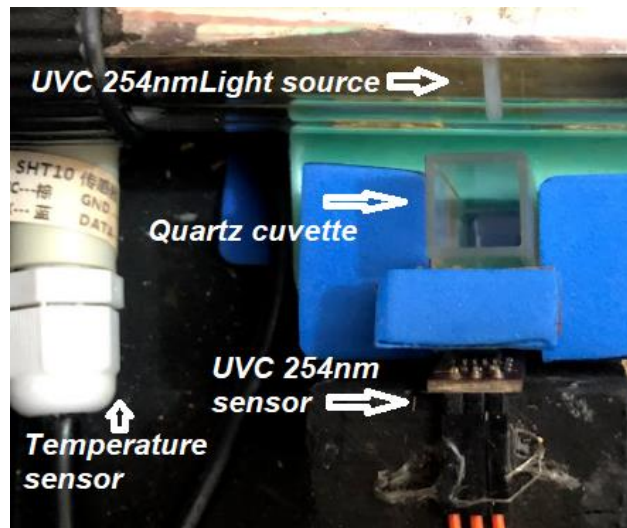


Fig. 5 - Chamber for 254 nm UVC transmittance measurement

**RESULTS**

The temperature range in which the UVC-254 nm measurements were taken was between 5°C and 30°C, to determine if this variation influences the UVC-254 measurements for each state of charge, an analysis of both values was performed for all the states of charge worked (See Fig. 6) (Each combination corresponds to a test of the SOH in each of the cells during the wear process.). And it was obtained by statistical analysis that the correlation and the P-value (which indicates whether a statistical value is possible from a certain null hypothesis) show that there is no relationship between the variables for the interval investigated.

If P is less than the significance level (the default value is =0.05), the corresponding correlation in R is considered significant, in this case the correlation was close to zero (0.0803) and the value gave a value of 19% indicating no relationship or no significance of the correlation between the variables for which there is then no dependence between the variables analysed (Temperature and UVC-254). And the subsequent analysis is performed without considering the temperature parameter for the range of 25°C to 30°C.

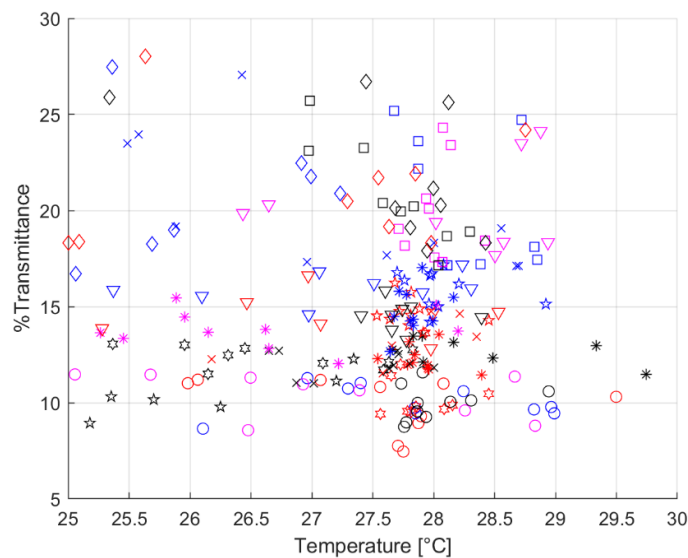


Fig. 6 - Dispersion of the points tested for transmittance and temperature around the measurement chamber.

The other aspect to consider when collecting transmittance samples for each state of charge is to ensure that the battery is at 100% charge since there is a relationship between the transmittance of a discharged battery and a charged one.

Fig. 7 shows the maximum variation of the UVC-254 nm transmittance when the battery is charged and discharged for each of the 4 cells tested, when the battery health state was at 57.62%.

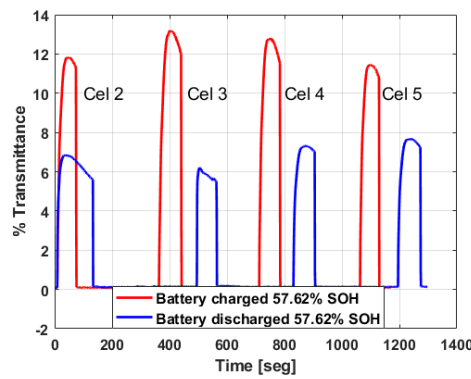


Fig. 7 - Values for % transmittance in a charged and discharged battery electrolyte

The study was performed on 4 batteries of 42 Ah which were subjected to continuous charge and discharge cycles to reduce the capacity or SOH, the depth of discharge was 100% taking as total discharge when the battery presented 10.5 V, the discharge cycles were performed at a rate of 14.2% of the maximum capacity (6 A) during several cycles, until reaching SOH values of: 30.5%, 32.9%, 40%, 49.8%, 52.6%, 57.6%, 71%, 79.5%, 86.2%, 94.8%, 95.7%, 99.2%, and 100%. Four replicates were performed for each battery represented by each of the cells (the cells at the ends of the battery were not taken into account to avoid the error of their contact with the plastic container) and five replicates were performed per replicate (for a total of 260 measured data). The distribution of the values obtained for all the data and for the data with the averaged replicates are shown in Figs. 8 and 9, respectively.

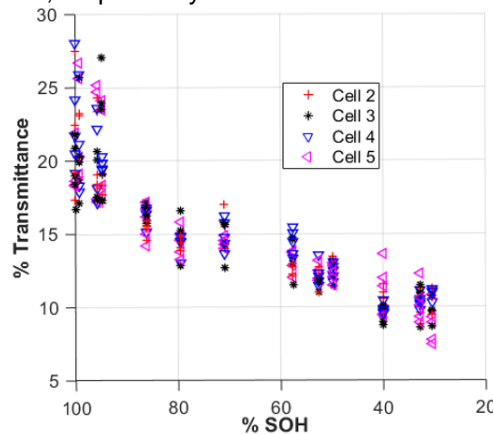


Fig. 8 - Distribution of the point cloud for each of the SOH measurements for each of the reported transmittance percentages

Although the average values at different health states for each cell overlap (Fig. 9.a), the transmittance values between health state ranges decrease as the batteries lose their health state, becoming well defined in health state ranges, as shown enclosed in black ovals in Fig. 9.b; even between these ranges the transmittance values do not overlap, making this novel method a powerful tool for qualitatively and quantitatively determining the loss of lead-acid battery life.

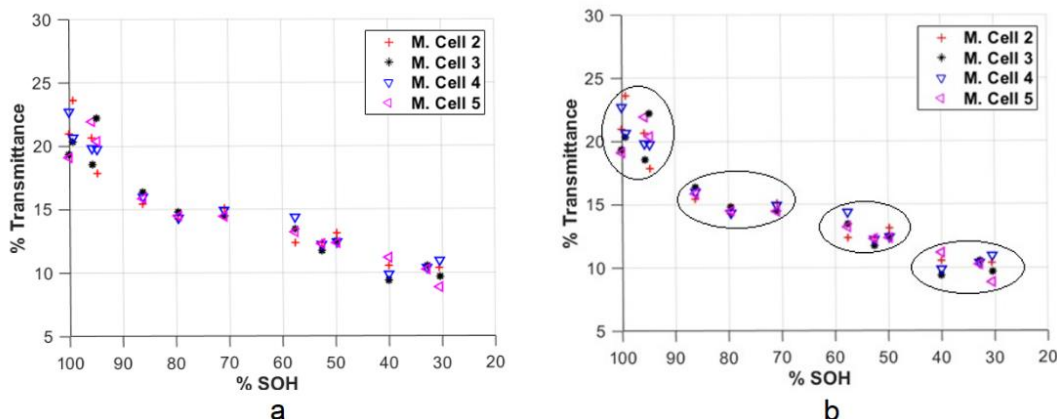


Fig. 9 - Averaged values of the 5 repetitions for SOH with the respective transmittance reported

The average transmittance values of the 13 SOH points measured in their different replicates and repetitions are shown in Table 1. This table shows the variation between the values for the battery with minimum SOH or maximum wear analysed (Group 1) and the values for the same battery when it was new (Group 4).

Table 1

**Transmittance value for all the replicates and replicates tested separated and the tested replicates separated by groups**

SOH	Group	Transmittance
[%]		[%]
30.5	1	9.97
32.9		10.41
40		10.26
49.8	2	12.61
52.6		12.14
57.6		13.35
71	3	14.75
79.5		14.47
86.2		15.91
94.8	4	20.06
95.7		20.26
99.2		25.75
100		20.54

## CONCLUSIONS

The SOH measurement system addressed in this work has not been seen developed by other researchers in any reference found, presenting it as a new methodology for SOH measurement; moreover, the results are conclusive observing that as the battery ages, the electrolyte presents a variation in its concentration that opposes the passage of UVC light, no water is added to the electrolyte so as not to bias the SOH measurement. Although the relationship of the decrease in transmittance with SOH is not linear, they present well determined variations for SOH ranges worked.

## ACKNOWLEDGEMENT

Part of the resources of this project has been financed by the Tesla research group of the Universidad of Antioquia and the direction of technology and innovation of the Institución Universitaria Pascual Bravo.

## REFERENCES

- [1] Bercibar, M., Gandiaga, I., Villarreal, I., Omar, N., Van Mierlo, J., & Van Den Bossche, P. (2016). Critical review of state of health estimation methods of Li-ion batteries for real applications. *Renewable and Sustainable Energy Reviews*, 56, 572–587. <https://doi.org/10.1016/j.rser.2015.11.042>
- [2] Bhardwaj, S. K., Singh, H., Deep, A., Khatri, M., Bhaumik, J., Kim, K. H., & Bhardwaj, N. (2021). UVC-based photoinactivation as an efficient tool to control the transmission of coronaviruses. *Science of the Total Environment*, 792, 148548. <https://doi.org/10.1016/j.scitotenv.2021.148548>
- [3] Dey, S., Ayalew, B., & Pisu, P. (2014). Combined estimation of State-of-Charge and State-of-Health of Li-ion battery cells using SMO on electrochemical model. *Proceedings of IEEE Workshop on Applications of Computer Vision*. <https://doi.org/10.1109/VSS.2014.6881140>
- [4] Gaouzi, K., El Fadil, H., Rachid, A., Lassioui, A., El Idrissi, Z., & Giri, F. (2021). Sampled-Data Observer for Estimating the State of Charge, State of Health, and Temperature of Batteries. *Electric Power Components and Systems*, 48(19–20), 2168–2180. <https://doi.org/10.1080/15325008.2021.1913262>
- [5] García Quintero, E., & Palacio-Fernández, J. A. (2020). Development of an electronic load applied to the characterization of electric batteries. *International Journal of Engineering Research and Technology*, 13(5), 973–977. <https://doi.org/10.37624/ijert/13.5.2020.973-977>

- [6] Heßling, M., Hönes, K., Vatter, P., & Lingenfelder, C. (2020). Ultraviolet irradiation doses for coronavirus inactivation – review and analysis of coronavirus photoinactivation studies. *GMS Hygiene and Infection Control*, 15, 1–8. <https://doi.org/10.3205/DGKH000343>
- [7] Ng, K. S., Moo, C. S., Chen, Y. P., & Hsieh, Y. C. (2009). Enhanced coulomb counting method for estimating state-of-charge and state-of-health of lithium-ion batteries. *Applied Energy*, 86(9), 1506–1511. <https://doi.org/10.1016/j.apenergy.2008.11.021>
- [8] Olabi, A. G., Onumaegbu, C., Wilberforce, T., Ramadan, M., Abdelkareem, M. A., & Al – Alami, A. H. (2021). Critical review of energy storage systems. *Energy*, 214, 118987. <https://doi.org/10.1016/j.energy.2020.118987>
- [9] Olia, H., Torabi, M., Bahiraei, M., Ahmadi, M. H., Goodarzi, M., & Safaei, M. R. (2019). Application of nanofluids in thermal performance enhancement of parabolic trough solar collector: State-of-the-art. *Applied Sciences (Switzerland)*, 9(3). <https://doi.org/10.3390/app9030463>
- [10] Ospina Agudelo, B., Zamboni, W., & Monmasson, E. (2021). *Application domain extension of incremental capacity-based battery SoH indicators*. *Energy*, 234, 121224. <https://doi.org/10.1016/j.energy.2021.121224>
- [11] Rezvanizani, S. M., Liu, Z., Chen, Y., & Lee, J. (2014). *Review and recent advances in battery health monitoring and prognostics technologies for electric vehicle (EV) safety and mobility*. *Journal of Power Sources*, 256, 110–124. <https://doi.org/10.1016/j.jpowsour.2014.01.085>
- [12] Suozzo, B. (2008), *Lead acid battery aging and state of health diagnosis*. B.S. thesis, The Ohio State University.
- [13] Takeda, F., Janisiewicz, W., Short, B., Leskey, T., & Stager, A. (2021). Ultraviolet-C (UV-C) for disease and pest management and automating UV-C delivery technology for strawberry. *Acta Horticulturae*, 1309(April), 533–541. <https://doi.org/10.17660/ActaHortic.2021.1309.76>
- [14] Wang, P., & Zhu, C. (2020). Summary of Lead-acid Battery Management System. *IOP Conference Series: Earth and Environmental Science*, 440(2). <https://doi.org/10.1088/1755-1315/440/2/022014>
- [15] Wong, Y. W., Chong, L. W., Rajkumar, R. K., Leng, W. Y., & Rajkumar, R. K. (2017). A new state-of-charge estimation method for valve regulated lead acid batteries. *Journal of Engineering Science and Technology*, 12(3), 584–595.
- [16] Xiong, R., Li, L., & Tian, J. (2018). Towards a smarter battery management system: A critical review on battery state of health monitoring methods. *Journal of Power Sources*, 405(5), 18–29. <https://doi.org/10.1016/j.jpowsour.2018.10.019>